Breast Cancer: Basic and Clinical Research

ORIGINAL RESEARCH

ODAM Expression Inhibits Human Breast Cancer Tumorigenesis

Daniel P. Kestler[1], James S. Foster[1], Charles T. Bruker[2], John W. Prenshaw[3], Stephen J. Kennel[1], Jonathan S. Wall[1], Deborah T. Weiss[1] and Alan Solomon[1]

[1]Human Immunology and Cancer Program/Department of Medicine, [2]Department of Pathology, University of Tennessee Graduate School of Medicine, Knoxville, Tennessee, USA. [3]University of Tennessee College of Medicine, Memphis, Tennessee, USA. Corresponding author email: asolomon@utmck.edu

Abstract: We have posited that Odontogenic Ameloblast Associated Protein (ODAM) serves as a novel prognostic biomarker in breast cancer and now have investigated its potential role in regulating tumor growth and metastasis. Human breast cancer MDA-MB-231 cells were transfected with a recombinant *ODAM* plasmid construct (or, as a control, the plasmid vector alone). ODAM expression increased adhesion and apoptosis of the transfected MDA-MB-231 cells and suppressed their growth rate, migratory activity, and capability to invade extracellular matrix-coated membranes. Implantation of such cells into mouse mammary fat pads resulted in significantly smaller tumors than occurred in animals that received control cells; furthermore, ODAM-expressing cells, when injected intravenously into mice, failed to metastasize, whereas the control-transfected counterparts produced extensive lung lesions. Our finding that induction of ODAM expression in human breast cancer cells markedly inhibited their neoplastic properties provides further evidence for the regulatory role of this molecule in tumorigenesis and, consequently, is of potential clinical import.

Keywords: invasion, cell adhesion, cell aggregation, breast tumor cell inhibition, tumor imaging

Breast Cancer: Basic and Clinical Research 2011:5 73–85

doi: 10.4137/BCBCR.S6859

This article is available from http://www.la-press.com.

Introduction

Breast malignancies are a leading cause of female cancer-related deaths in the United States, with an estimated world-wide mortality of over 40,000 individuals in 2010.[1] Progress in reducing the societal impact of this disease has been limited due to its biological and pathological diversity, as manifested by distinct phenotypes, differences in prognosis, and response to therapy.[2] The heterogeneous nature of breast cancer has been attributed to the variability in expression of genes that control cell growth and malignant potential[3,4] and, in this regard, we have reported[5] that the protein product of a gene involved in dental development[6,7]—Odontogenic Ameloblast Associated Protein (ODAM)—is expressed in certain human epithelial neoplasms, including breast cancer. Notably, this molecule appears to serve as a novel, favorable prognostic biomarker of this malignancy, as demonstrated by the finding of a statistically significant correlation between the nuclear presence of ODAM and an improved 5-year survival of patients, irrespective of disease stage.[8]

To gain further insight into the function of ODAM and to determine if its upregulation has a protective role in carcinogenesis, we transfected highly invasive ODAM-negative human breast cancer cells, MDA-MB-231,[9] with a cytomegalovirus promoter-based plasmid construct encoding for ODAM. We now report the results of our in vitro and in vivo studies which have shown that increased ODAM expression profoundly suppressed the neoplastic properties of these cells and, as such, may represent a novel and targeted form of therapy in patients with breast cancer.

Methods

Cell lines and tissue culture

The human breast cancer cell lines MDA-MB-231, T-47D, and MCF-7 were obtained from the American Type Culture Collection and maintained in a humidified chamber at 37 °C under 5% CO_2 with DMEM/F12 Hepes medium (Lonza) containing 5% fetal bovine serum (FBS, Invitrogen), penicillin (100 units/mL), and streptomycin (100 µg/mL). Hela and A549 cells were also obtained from ATCC and maintained similarly.

Recombinant human ODAM

A full-length recombinant (r) human ODAM-pcDNA5T/O (Invitrogen) plasmid construct, which included the leader coding sequence, was generated using Phusion thermal polymerase (New England Biolabs) by PCR extension of a pSmart r-human ODAM cloned insert encoding the 279-residue mature protein, plus c-terminal FLAG and 8XHis epitopes.[5] The product was gel purified, inserted into the EcoRV position of the pcDNA5T/O multiple cloning site, and the nucleotide sequence of the resultant product determined at the University of Tennessee's Molecular Biology Core facility.

Transfection of breast cancer cells with rODAM

MDA-MB-231 cells were transfected with either a human ODAM-pcDNA5T/O construct or, as a control, the vector alone, using Lipofectamine LTX reagent (Invitrogen) according to the manufacturer's protocol. Growth selection was performed with hygromycin (400 µg/mL) in 100-mm culture dishes and visible colonies were transferred into 24-well plates. After 7 to 10 days, the media were tested for ODAM production by capture ELISA (see below) and ODAM-positive and control cell clones (designated 231-ODAM or 231-CON, respectively) were expanded.

Capture ELISA screening for ODAM protein

For ODAM detection, 96-well polystyrene microtiter plates (Corning) were coated with the anti-ODAM monoclonal antibody (mAb) 5A1,[5] blocked with bovine serum albumin (BSA, Sigma-Aldrich), and filled with 200 µL of cell culture supernatant from putative ODAM-expressing clones. After a 1-h incubation at 37 °C, wells were washed with PBS/0.1% Tween 20 (Sigma-Aldrich), incubated with biotinylated anti-ODAM mAb 8B4 and, following further washes, exposed to peroxidase-conjugated streptavidin.[5] Finally, after addition of the ABTS peroxidase substrate, bound biotinylated anti-ODAM mAb was measured at 405 nm using a BioTek Synergy HT plate reader.

Detection of rODAM

Transfected cells were plated onto 22-mm glass coverslips (Fisher) in 6-well BD Falcon tissue culture plates (BD Biosciences) and, 72 h later, washed with PBS, fixed with 4% paraformaldehyde, permeabilized with

0.25% Triton X-100/PBS, and blocked with 3% BSA in PBS. To detect intracellular ODAM, the cells were exposed, first to mAb 8B4, and then to AlexaFluor488 goat anti-mouse IgG (Invitrogen); the cell nuclei were counterstained with Hoescht 33342 (Invitrogen). Cellular F-actin was visualized in fixed/permeabilized cells stained with AlexaFluor488-conjugated Phalloidin (Invitrogen) and Hoescht 33342.

Western blotting

For Western blots, supernatants from 72-h 231-CON and 231-ODAM cultures were centrifuged at 2000 × g to remove cellular debris and the rODAM bound via the HIS-tag to Co^{++}-iminodiacetic acid agarose resin was released with 50 mM EDTA. An aliquot was removed, electrophoresed on a 10% bis-Tris gel (Invitrogen), and ODAM detected using a combination of anti-ODAM mAbs 8B4 and 5 A1, as described previously.[5,10] For determination of Triton-soluble and total vimentin levels, cultured cells were washed in PBS and lysed either in a Triton buffer (20 mM Tris, pH 7.5, 150 mM NaCl, 0.5% Triton X-100, 0.5 mM PMSF) or in the same buffer supplemented with 0.5% deoxycholic acid and 0.1% sodium dodecyl sulfate (RIPA buffer), followed by centrifugation at 15,000 × g for 20 min at 4 °C.[11] Supernatants were electrophoresed and blotted using a mouse anti-vimentin mAb (sc-32322, Santa Cruz Biotech). As a control for detergent extraction of vimentin, the blot was stripped in glycine/SDS (pH, 2.5) and re-probed with an anti-β actin antibody (clone AC-74, Sigma).

Cell growth and aggregation assays

231-ODAM and 231-CON cells were trypsinized, counted, and plated in quadruplicate in 24-well tissue culture plates at a concentration of 1×10^4 cells/well. One, 4, 7, and 10 days later, cells were fixed by addition of 4% glutaraldehyde, washed with water, dried, and then stained with 0.1% crystal violet. After another wash and solubilization with 10% acetic acid, the cell content was measured by absorbance at 562 nm. Growth rates were determined by linear regression analysis using GraphPad Prism 4.0 software. For cell aggregation assays, subconfluent 231-CON and 231-ODAM cultures were treated with trypsin-EDTA (Lonza) for 15 min, washed twice in PBS, suspended in Hank's Balanced Salt Solution lacking Ca^{++} and Mg^{++} (Lonza), and plated at 1×10^5 cells/mL in 1% agar-coated 6-well tissue culture plates. After incubation for 3 h at 37 °C on a rotating shaker set at 80 rpm, the extent of aggregation was visualized microscopically and multiple representative fields were photographed for comparative purposes.

BrdU labeling

231-ODAM and 231-CON cells were trypsinized and plated at 2×10^5 cells/well on 22-mm glass coverslips (Fisher) in 6-well tissue culture plates (BD Falcon). After 3 days, the cultures were pulsed for 3 h with 50 μM BrdU (Sigma-Aldrich), fixed with cold 70% ethanol, and blocked by addition of 3% BSA. Cellular DNA was denatured with 2 N HCl/0.5% Triton X-100, followed by 3 PBS washes. Intracellular incorporation of BrdU was detected using an AlexaFluor488-conjugated anti-BrdU antibody (Invitrogen); nuclei were counterstained with Hoescht 33342. Six representative 200× fields containing >1000 cells from each group were photographed and the labeled versus unlabeled nuclei counted.

Apoptosis assays

231-ODAM and 231-CON cells were plated at a range of cell densities to yield (at 72 h) high density (1.2×10^5 cells/cm^2) and low density (3×10^4 cells/cm^2) cultures. The extent of apoptosis was determined by measurement of soluble chromatin, using a Cell Death Detection ELISA (Roche Diagnostics) as described by the manufacturer. After staining with Annexin V-FITC/propidium iodide (BD Biosciences), the percentage of apoptotic cells present in the high density cultures was quantitated by flow cytometry using a Becton Dickinson FACScan flow cytometer; data from a minimum of 5000 events were collected in 2 separate experiments. For determination of caspase-3 activation, 231-ODAM and 231-CON cells from the high-density cultures were lysed in 10 mM Tris-PBS, pH 7.6 containing 1% Triton X-100 and 10 mM sodium pyrophosphate. Five μL of the lysate were added to 100 μL of the assay buffer (10 mM Hepes, pH 7.5/10% glycerol/2 mM dithiothreitol) containing 20 μM of the fluorogenic caspase-3 substrate Ac-DEVD-AMC (BD Biosciences), as per manufacturer's instructions. After 1-h incubation at 37 °C, the fluorescent product was measured in a BioTek Synergy HT plate reader (excitation and emission wavelengths, 360 and 440 nm, respectively).

Cell-substrate adhesion assays

Polystyrene 96-well tissue culture plates were coated overnight at 4 °C with 50 µL/well of either Matrigel (Becton Dickinson), Type IV collagen (Sigma-Aldrich), or BSA, each at a concentration of 50 µg/mL. After washing with PBS, the wells were filled with 50 µL of suspended, trypsinized 231-ODAM or control cells (5×10^5 cells/mL) and the plates incubated at 37 °C for 40 min.[12] After washing with PBS, the cells were fixed for 30 min with 4% glutaraldehyde and washed with water. The number of bound cells was determined after staining with 0.1% crystal violet and solubilization with 10% acetic acid by measurement of the amount of dye released (absorbance, 562 nm).[13] To correct for non-specific binding, the average absorbance values in BSA-coated wells were subtracted from those derived experimentally.

Cell migration and invasion assays

Trypsinized 231-ODAM and 231-CON cells were washed and suspended (1×10^6 cells/mL) in serum-free DMEM/F12 medium and a 100 µL aliquot was placed in the upper chamber of a Costar Transwell permeable support (8-µm pore size); the lower chamber was filled with 0.7 mL of DMEM/F12 medium with 10% FBS serving as a chemoattractant. After incubation at 37 °C for 18 h, the membrane was fixed in ethanol and stained with HEMA3 Wright-Giemsa (Fisher Scientific). Non-migrating cells were swabbed from the upper surface and those that passed through to the lower surface were photographed and counted.[11] For barrier invasion assays, membranes were pre-coated with 40 µL of Matrigel (0.25 mg/mL) and assayed as above for cell migration.

In vivo studies

All animal experiments were conducted in accordance with United States Public Health Service guidelines and under the auspices of protocols approved by the University of Tennessee's Animal Care and Use Committee.

Xenografts of trypsinized, washed 231-ODAM and 231-CON cells suspended in PBS (3×10^7 cells/mL) containing 50% Matrigel were established in groups of 5 severe combined immunodeficient (SCID)-beige 9-wk old female mice (Charles River) or Rag-1 immunodeficient mice (from the University of Tennessee Graduate School of Medicine mouse colony) by 100-µL subcutaneous injections into the right inguinal mammary fat pads. Six wks later, the animals were euthanized and the tumors were removed, weighed, fixed in formalin, and embedded in paraffin blocks. To determine the metastatic potential of the cells, similar groups of mice were given, via tail vein, injections of 8×10^5 cells. Thirty-one days later, the animals were imaged by PET/CT (see below) and lung tissue harvested for microscopic and immunohistochemical examination.

Tumor imaging

3'deoxy-3'[^{18}F-fluoro-thymidine] (^{18}FLT) was synthesized using the Advion NanoTek LF flow-based microfluidic chemistry system.[14] Mice were injected in the lateral tail vein with ~200 µCi of radiotracer in 200 µL PBS containing <10% ethanol, and 1-h later, after sacrifice by isoflurane inhalation overdose, PET and CT images were generated using an Inveon Trimodality SPECT/PET/CT scanner. PET data were acquired over 15 min and reconstructed by means of the iterative maximum a posteriori (MAP) algorithm with a zoom and b-factor of 2 and 0.001, respectively. CT data were collected using 360 azimuths over 360° of rotation with an exposure time of 240 msec. The X-ray voltage and current were 80 kVp and 500 µA, respectively. Images were reconstructed with a filtered backprojection algorithm on a 2048 × 3072 matrix with an effective voxel size of 55 µm. PET and CT images were co-registered automatically and analyzed using the Inveon Research Workplace software (Siemens Preclinical Solutions).

Immunohistochemistry

Four µm-thick formalin-fixed, paraffin embedded tissue sections were mounted on poly-L-lysine-coated slides, dried overnight at room temperature, and deparaffinized. Slides were immersed in Glyca pH 4.0 antigen–retrieval solution (BioGenex), heated in a microwave oven, and immunostained with the anti-ODAM mAb 8B4, using the ImmPRESS polymerized reporter enzyme-linked system (Vector Laboratories), as previously described.[15] Ki-67 expression was determined utilizing the MIB-1 anti-Ki-67 antibody (Dako) and the number of positive nuclei in the most active growth regions of the tumors enumerated in 4 representative 200× fields from each of 5 mice.[16] Active caspase-3 expression was visualized with

a rabbit anti-cleaved caspase-3 (Asp175) polyclonal antibody (Cell Signaling Technology).

Transient transfection assays of cell proliferation and apoptosis

MDA-MB-231 and MCF-7 cells were cultured in 24-well plates or on 15-mm coverslips at ~30% confluency and transfected with 1 µg/well of the ODAM-pcDNA5T/O or control vector, each in combination with 0.15 µg of pEGFPN1 vector (Clontech) as a marker of cell transfection. After 72 h incubation, 24 well cultures were assayed for apoptosis by ELISA as above. Cells on cover slips were labeled for 2 h with BrdU and its incorporation in transfected cells analyzed by co-staining GFP and BrdU using rabbit anti-GFP and AlexaFluor594-conjugated anti-rabbit antibodies (Invitrogen) and AlexaFluor488-conjugated anti-BrdU. BrdU-positive nuclei were counted as a fraction of GFP-positive cells in 9 fields for each transfected culture.

Results

Induction of ODAM expression in human breast cancer cells

Human r-ODAM (containing the full coding sequences including the secretory leader plus 3'-FLAG and −8XHis epitopes) was transiently expressed as a pcDNA5/TO construct in MDA-MB-231, MCF-7, and Hela cells, as evidenced immunocytologically and by an ELISA of culture fluid supernatants. This protein was not detected in control vector-transfected or untreated cells. As seen in Table S1 (*see* supplemental data), only one cell line, MDA-MB-231, was capable of sustained ODAM expression after antibiotic selection. In contrast, 4 different human neoplastic cell lines (including 2 others of breast origin) showed no evidence of continued rODAM expression.

As illustrated in Figure 1A, cells from the most prolific MDA-MB-231 clone (#32), designated 231-ODAM, were immunostained by the anti-ODAM specific mAb 8B4 at the cell matrix/border, as well as the nuclear/paranuclear regions, presumably in the Golgi apparatus. Additionally, 5 to 10 ng/mL of ODAM was detected by capture ELISA in culture fluid supernatants from cells grown to confluency. Its presence also was revealed by Western blot analysis of the media, albeit at a higher than predicted molecular mass (49 versus 29 kDa) due to glycosylation (Fig. 1B).[6]

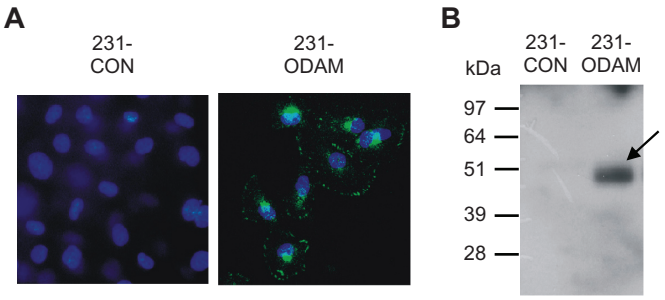

Figure 1. Recombinant ODAM expression in MDA-MB-231 breast cancer cells. **A**) Reactivity (green immunofluorescence) of anti-ODAM mAb 8B4 with Hoechst 33342-stained control vector (231-CON) and ODAM-transfected (231-ODAM) cells (original magnification, ×400). **B**) Western blot analysis of 231-ODAM clone #32 culture fluid supernatant (the M_r markers are as indicated).

Notably, there was no evidence in the immunoassays of ODAM expression by vector-only transfected cells (designated 231-CON).

Effect of ODAM expression on properties of human breast cancer cells

In a series of in vitro experiments, we compared the properties of cells obtained from the stably transfected 231-ODAM clone #32 with those of plasmid vector-transfected controls. The number of ODAM-expressing cells was 4-fold less than that of the controls after 10 days in culture (Fig. 2A), as also shown with a second 231-ODAM clone (supplemental Fig. S1A). Further, their low growth rate was evidenced by limited incorporation of BrdU (Fig. 2B). ODAM-expressing MDA-MB-231 cells had an increased rate of apoptosis relative to control cultures, especially at higher cell densities where the apoptotic fraction in 231-ODAM cultures was found to be ~2.5 times that of the controls (Fig. 2C, D). This effect was associated with a demonstrable increase in caspase-3 activation (Fig. 2E). Transient transfection assays indicated that ODAM expression inhibited MCF-7 cell proliferation by 48%, as measured by BrdU incorporation after 72 h, and to a lesser degree, that of MDA-MB-231 cells (31%) (Supplemental Fig. S2A). Transient ODAM expression also increased by four-fold the extent of apoptosis in MCF-7 cells (Supplemental Fig. S2B), whereas this effect did not occur with MDA-MB-231 cells.

The results of studies (Fig. 3A) measuring the binding of 231-ODAM cells to Matrigel- or type IV collagen-coated plates revealed significantly greater attachment ($P < 0.01$) than did the 231-CON cells.

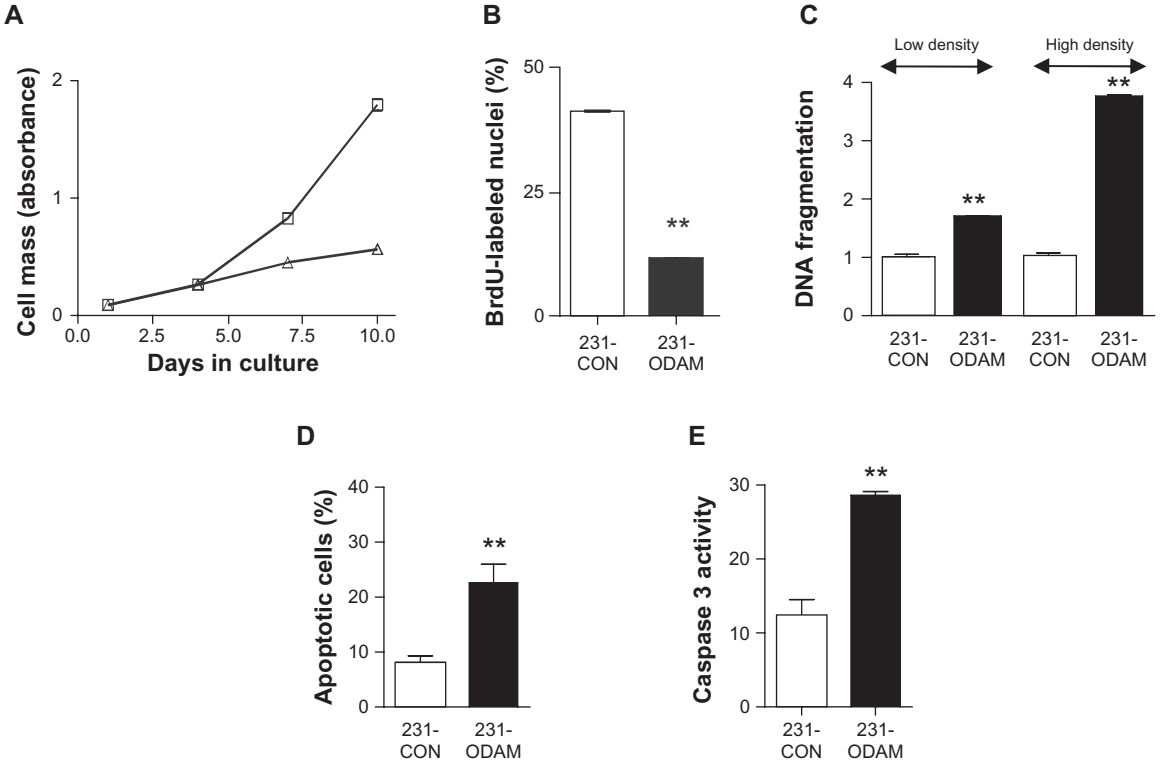

Figure 2. ODAM expression inhibits growth and elicits apoptosis of MDA-MB-231 cells. **A**) Growth rates of 231-CON (□) and 231-ODAM (Δ) cells. Plotted values represent absorbance and are given as mean ± 1 standard deviation for 4 replicates. **B**) DNA replication in 231-CON and 231-ODAM cultures, as depicted as percent of BrdU-labeled nuclei. Data are given as the mean ± 1 standard deviation (**$P < 0.01$) as measured in 6 fields from 2 independent cultures (>1000 cells). **C**) Relative apoptosis in low- and high-density cultures of 231-CON and 231-ODAM cells. Determinations were based on a soluble chromatin ELISA where the values are given as the mean ± 1 standard deviation (**$P < 0.01$) from triplicate cultures. **D**) Apoptotic fractions in high density cultures of 231-CON and 231-ODAM cells based on Annexin V staining. Values are given as the mean ± 1 standard deviation (**$P < 0.05$) from 2 independent experiments. **E**) Caspase-3 activation in 231-CON and 231-ODAM cells. Values for the extent of fluorogenic caspase-3 substrate cleavage are given as the mean ± 1 standard deviation (**$P < 0.01$) from triplicate cultures.

ODAM expression in MDA-MB-231 cells also elicited a significant increase in their ability to form cell aggregates (Fig. 3B and Fig. S1B). Analysis of F-actin organization by phalloidin staining (Fig. 4A) revealed rearrangement of the visible stress fibers to circumferential cables.[17–19] Additionally, ODAM expression resulted, not only in a striking increase in soluble vimentin (whereas overall vimentin levels were unchanged, Fig. 4B), but also decreased, by ~50% ($P < 0.01$), the capability of these cells to migrate towards a chemoattractant, (Fig. 5A), as well as penetrate and invade a Matrigel barrier (Fig. 5B).

Effect of ODAM expression on the neoplastic potential of human breast cancer cells

To determine if ODAM expression would affect the aggressive tumor-forming and metastatic properties of MDA-MB-231 cells in vivo,[9] 231-ODAM and control cells (3×10^6) were suspended in 50% Matrigel and injected into the inguinal mammary fat pads of SCID-beige mice (5 per group). Within 6 wks, the tumors in those animals that received the control cells had grown to ~1 cm, whereas those formed by the ODAM-transfected counterparts were ~16-fold smaller in size and, in some cases, barely detectable (Fig. 6A). Additionally, they had considerably reduced Ki-67 expression (31% versus 83%; $P < 0.01$; Fig. 6B) and caspase-3 was readily detected in localized areas of the 231-ODAM xenografts while, in the 231-CON tumors, only rare, single cells contained the activated enzyme (Fig. 6C). Similarly, the growth of tumors generated from injection of MDA-MB-231 ODAM-transfected cells (clones 32 and 20) into a second immunocompromised animal, ie, Rag-1 mice, was comparably inhibited, as shown in Figure S1C.

In other experiments, groups of SCID mice were given intravenous injections of 8×10^5 ODAM-transfected or control MDA-MB-231 cells. By 31 days, the latter animals were in obvious distress

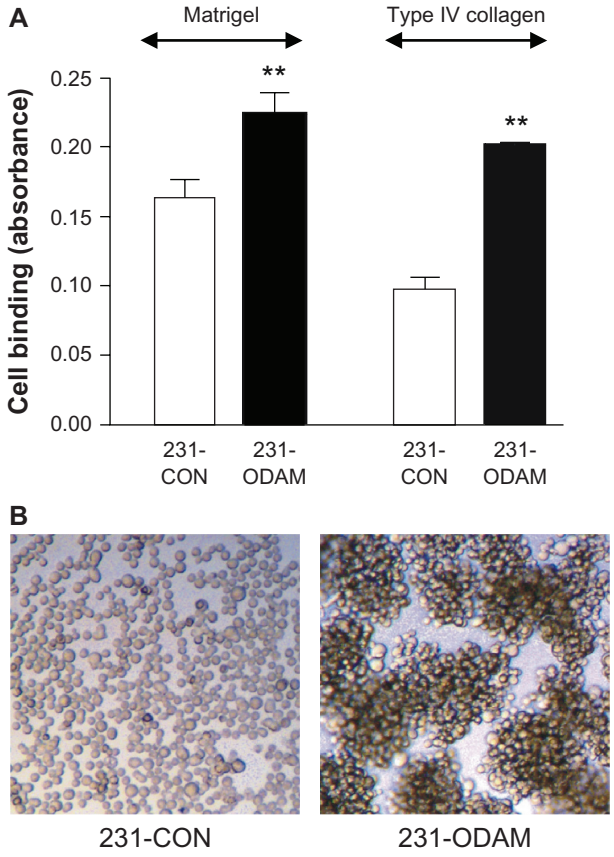

Figure 3. ODAM expression in MDA-MB-231 cells promotes adhesion to protein matrices and cell-cell aggregation. **A**) Adhesion of 231-CON (light bars) and 231-ODAM (dark bars) cells to Matrigel or Type IV collagen-coated plastic surfaces. Binding values are based on absorbance of adherent cells and are given as the mean ± 1 standard deviation for 10 replicates (**$P < 0.01$). **B**) Cell-cell aggregation of trypsinized 231-CON and 231-ODAM cells after 3 h in suspension culture (original magnification, ×40).

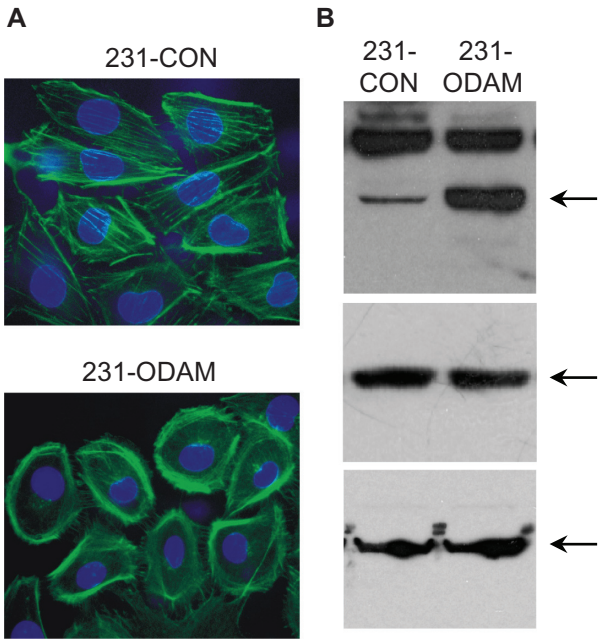

Figure 4. ODAM expression elicits cytoskeletal rearrangement in MDA-MB-231 cells. **A**) F-actin arrangement in 231-CON and 231-ODAM cells was visualized by Phalloidin staining (green) with nuclei counterstained (blue); original magnifications, ×400). **B**) Western blot detection of Triton X-soluble vimentin (top panel), soluble β-actin (middle panel), and total vimentin (bottom panel) in 231-CON and 231-ODAM cultures.

due to extensive multinodular pulmonary metastases that were metabolically active, as evidenced by ^{18}FLT micro-PET/CT scans (Fig. 7A). In contrast, those that received the 231-ODAM cells essentially had no lung lesions by imaging. The mean activities measured in 0.4 mm^3 areas of interest in the lungs were 0.643 MBq/cm^3 for 231-CON [n = 1] and 0.083 ± 0.062 MBq/cm^3 [n = 3] for 231-ODAM recipients. In necropsy sections of mice receiving 231-ODAM cells only rare tumor deposits were found lodged in alveolar septal capillaries, with no evidence of invasion, and a complete lack of fibrosis, desmoplasia, or other host response (Fig. 7B).

Discussion

Historically, a portion of the gene encoding ODAM was recognized initially through the Japanese NEDO human cDNA-sequencing project where messenger RNA specifying the C-terminal 153 amino acids was cloned from the KATO III signet-ring gastric carcinoma cell line.[20] Subsequently, the coding sequence representing the entire 279-residue protein was identified and homologous nucleotide sequences were detected in certain fetal and adult tissues.[21] The first evidence of the expressed protein resulted from our analyses of amyloid associated with calcifying epithelial odontogenic (Pindborg) tumors, where the fibrils were found to consist of ODAM-related peptides.[22,23] Although the biological function of ODAM has not been established, it undoubtedly has a fundamental role in odontogenesis[6,7] and is upregulated in human gastric cancers.[5,24]

To gain further insight into the potential role of ODAM expression in tissue development and carcinogenesis, we generated mAbs specific for this protein and demonstrated that these reagents recognized ODAM molecules, not only in ameloblasts, but also in certain normal epithelial and malignant tissues, especially those of breast origin where its presence was detected at the molecular level through RNA and in situ hybridization analyses.[5] Further, we found in a retrospective study of archival breast cancer specimens that patients whose tumor cells expressed nuclear

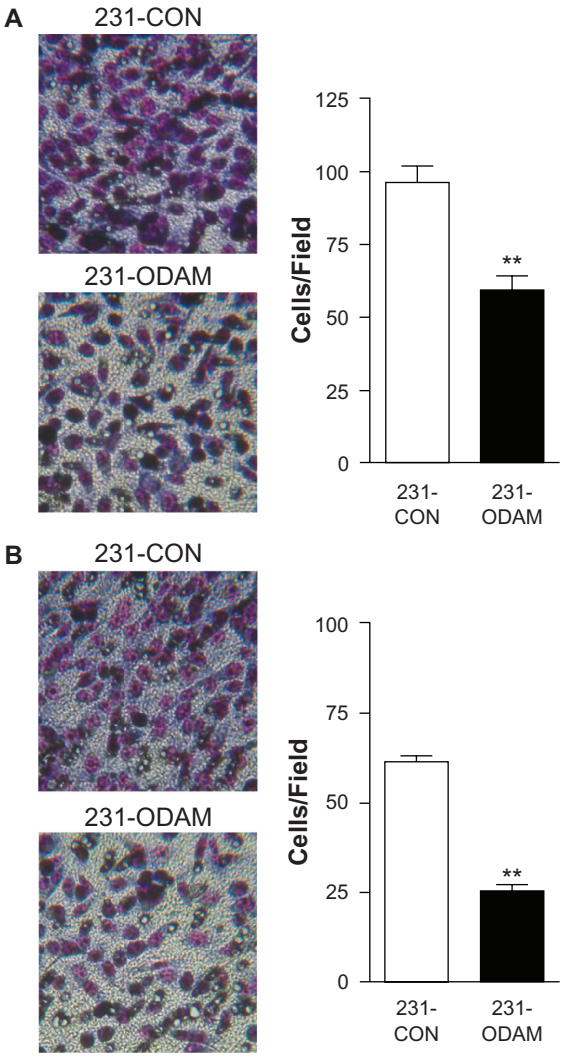

Figure 5. ODAM expression inhibits migration and Matrigel-barrier invasion of MDA-MB-231 cells. **A**) Transwell migration of 231-CON and 231-ODAM cells (Wright-Giemsa, original magnifications, ×200). **B**) Matrigel-barrier invasion of 231-CON and 231-ODAM cells. Undersides of Matrigel-coated, Wright-Giemsa-stained Transwell membranes (cell counts from 8 representative fields are given as the mean ± 1 standard deviation [$^{**}P < 0.001$]).

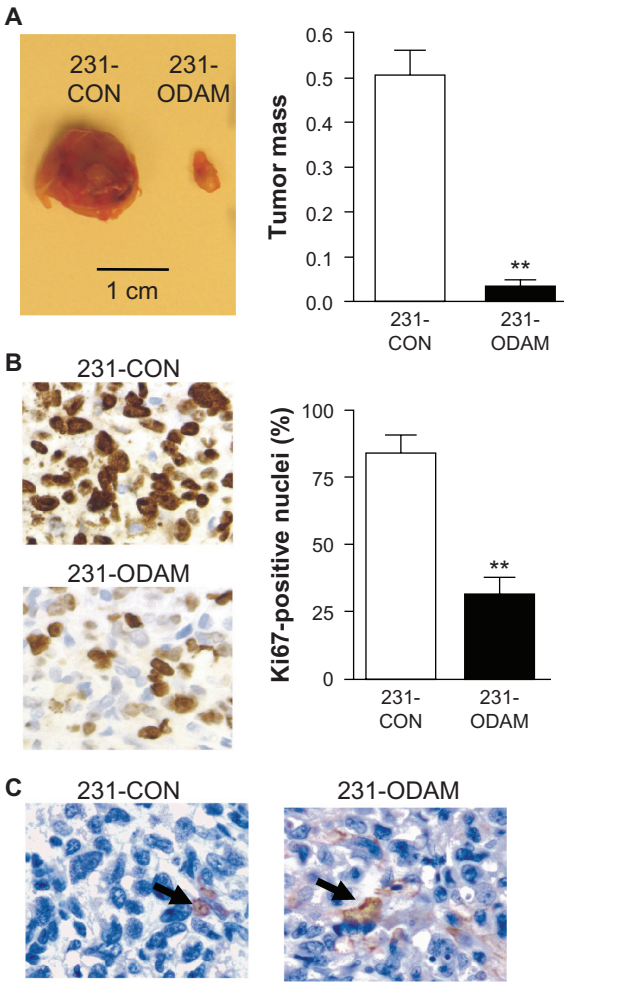

Figure 6. ODAM expression suppresses the development in mice of MDA-MB-231 solid tumor xenografts. **A**) Tumors harvested from the right mammary fat pads of SCID beige mice 6 wks after implantation of 3×10^6 231-CON or 231-ODAM cells in 50% Matrigel. Graphic representation of average tumor masses from 5 mice in each group ± 1 standard deviation ($^{**}P < 0.001$). **B**) Ki-67 expression in 231-CON and 231-ODAM tumors (original magnifications, × 200). Graphic representation of the percentage of Ki-67-positive nuclei in the 2 types of xenografts, as determined from 5 representative fields ($^{**}P < 0.01$). **C**) Activated caspase-3 in 231-CON and 231-ODAM tumors (original magnifications, ×200).

ODAM had an improved survival rate, irrespective of disease stage.[8]

Based on our results, we posit that ODAM expression may have a mitigating effect in breast neoplasia. When the highly aggressive human breast cancer cells MDA-MB-231[9] were transfected with a gene construct encoding this molecule, their tumorigenic properties were significantly lessened, ie, growth rate, migration, and invasiveness were reduced, while adhesion to extracellular matrices, cell-cell association, and rate of apoptosis were increased. Notably, these effects on cell proliferation and apoptosis also occurred upon transient expression of ODAM in MCF-7 human breast cancer cells indicating that these consequences of ODAM expression are not limited to MDA-MB-231 cells.

Strikingly, and in contrast to vector-only transfected controls, ODAM-positive MDA-MB-231 cells implanted into the mammary fat pads of SCID-beige mice grew at a significantly lower rate, resulting in harvested tumors of 16-fold lower mass. Furthermore, ODAM-transfected cells injected intravenously into the tail veins of SCID mice failed to form invasive lung metastases, as opposed to the extensive pulmonary lesions seen in recipients of the MDA-MB-231 vector-only control cells.

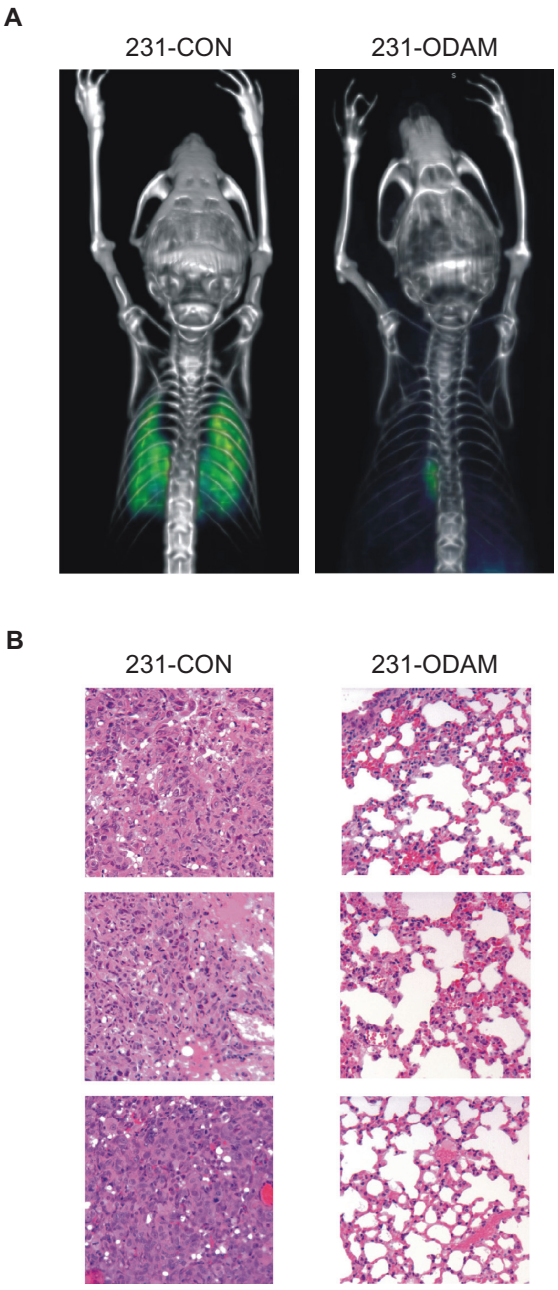

Figure 7. ODAM expression suppresses development in mice of MDA-MB-231 lung metastases. **A**) Representative volume-rendered, dorsal view images of ^{18}FLT accumulation (false colored green) in the lungs of 231-CON and 231-ODAM mice 31 days after intravenous injection of 8×10^5 cells. **B**) Representative hematoxylin/eosin-stained lung tissues from 231-CON and 231-ODAM injected mice (3 from each group, original magnifications, ×200).

We attribute the in vitro and in vivo reduction of tumorigenicity induced by ODAM expression, in part, to the role of this protein in modulating cellular junctional interactions and mobility.[6,25,26] In this regard, a number of other cell-adhesion molecules, eg, cadherins,[27] ZO-2,[28] profilin,[29] claudin,[30] and AF-6,[31] also have been shown to exhibit anti-tumor properties and, like ODAM, reside in the cytoplasm, nuclear/paranuclear regions, and at the cell surface.[32] Further, ODAM contains 6 PDZ-binding motifs that are found in several tight junction proteins, including VMP-1, JAM-A, claudin-4, and ZO, all of which have been implicated in malignant transformation, cell signaling, and specifically, breast tumor cell invasion.[28,30–37]

Ectopic expression of other genes, eg, *ER* (*p29*),[38] *KRT-18*,[39] *NET-6*,[40] or *sFRP1*,[41] has been shown to reduce proliferative potential and tumorigenicity in MDA-MB-231 human breast cancer cells through, for example, interference with the epithelial to mesenchymal transition of the tumor cells, upregulation of pro-apoptotic proteins, or attenuation of Wnt-pathway signaling by blockade of ligand binding.[5–7,8,31,42] ODAM shares a number of properties of the proteins encoded by these genes in that it is present in cell junctions and inhibits tumor cell growth, while enhancing apoptosis and promoting actin cable formation reflective of a more differentiated state.[18,19] However, ODAM is unique since it seemingly is limited to particular epithelial tissues and its secreted product is localized both to cell membrane/tissue interfaces and the nucleus, suggesting that this molecule has multiple regulatory functions.[5–8,31,42] Most notably, ODAM expression represents a favorable prognostic biomarker, as evidenced by our finding of lengthened survival in patients with breast cancer, regardless of tumor stage.[8]

The presence of ODAM in the nucleus has been reported to upregulate expression of matrix metalloproteinase MMP-20 by binding to its promoter region in cultured ameloblasts, while ODAM expression in these cells is, in turn, upregulated through interaction of the Runx2 transcription factor with the ODAM genomic promoter region.[43] Runx2 is expressed during normal mammary gland development, as well as in breast cancer where it is associated with bone metastases.[44–47] In addition, Runx2 activates the Indian Hedgehog pathway[48] and has been shown to interact directly with the Hedgehog-regulated Gli2 transcription factor.[49] Further, the related molecule, Gli-1, has been associated with adverse breast cancer prognosis and is expressed, along with ODAM, in breast, lung, and gastric tumors.[5,50–53] Additionally, inhibition of Runx2 expression in MDA-MB-231 cells results in loss of tumorigenicity.[44] The coactivator activator protein (CoAA) is a negative modulator of Runx2 that complexes with its DNA-binding domain and prevents

Runx2-mediated transcriptional activation of other genes resulting in effects similar to those exhibited by MDA-MB-231 cells after Runx2 inhibition.[44,54,55] Notably, ODAM contains 2 of these inhibitory Runx2-binding motifs that are found in CoAA. Thus, interactions of ODAM with Runx2 could contribute to suppression of the neoplastic properties of MDA-MB-231 cells. However, suppression of Runx2 in MDA-MB-231 cells has been shown to be limited to an anti-proliferative effect, whereas ODAM effects both proliferation and tumorigenicity, suggesting a broader role for ODAM in cellular development, renewal, and malignancy.[5–8,24,43,56,57]

In summary, our studies provide evidence for a functional role of this novel gene product, ODAM, in suppressing the growth rate, invasiveness, and metastatic potential of highly invasive human breast cancer cells. Given the favorable clinical prognosis that is associated with its expression by tumors, we posit that targeted upregulation of the *ODAM* gene may be of unique therapeutic benefit which could lead to a reduction in the morbidity and mortality associated with breast cancer and, possibly, other human epithelial malignancies.

Acknowledgements

We thank Sallie D. Macy, Craig Wooliver, and Charles L. Murphy for their technical support.

Current Support

Susan G. Komen Foundation for Breast Cancer Research and the Physicians Medical Research Foundation. A.S. is an American Cancer Society Clinical Research Professor.

Grant Support

Susan G. Komen Breast Cancer Foundation Grant #KG100384 and the Physicians Medical Research Foundation; A.S. is an American Cancer Society Clinical Research Professor.

Disclosure

This manuscript has been read and approved by all authors. This paper is unique and is not under consideration by any other publication and has not been published elsewhere. The authors and peer reviewers of this paper report no conflicts of interest. The authors confirm that they have permission to reproduce any copyrighted material.

References

1. Breast cancer facts and figures; 2009–2010. http://www.cancer.org/Research/CancerFactsFigures/breast-cancer-facts-figures-2009-2010.
2. Razzak AR, Lin NU, Winer EP. Heterogeneity of breast cancer and implications of adjuvant chemotherapy. *Breast Cancer*. 2008;15:31–4.
3. Leber MF, Efferth T. Molecular principles of cancer invasion and metastasis (review). *Int J Oncol*. 2009;34:881–95.
4. Anderson WF, Matsuno R. Breast cancterogeneity: a mixture of at least two main types? *J Natl Cancer Inst*. 2006;98:948–51.
5. Kestler DP, Foster JS, Macy SD, Murphy CL, Weiss DT, Solomon A. Expression of odontogenic ameloblast-associated protein (ODAM) in dental and other epithelial neoplasms. *Mol Med*. 2008;14:318–26.
6. Moffatt P, Smith CE, St-Arnaud R, Nanci A. Characterization of Apin, a secreted protein highly expressed in tooth-associated epithelia. *J Cell Bio Chem*. 2008;103:941–56.
7. Park JC, Park JT, Son HH, et al. The amyloid protein APin is highly expressed during enamel mineralization and maturation in rat incisors. *Eur J Oral Sci*. 2007;115:153–60.
8. Siddiqui S, Bruker CT, Kestler D, et al. Odontogenic ameloblast associated protein as a novel biomarker for human breast cancer. *Am Surg*. 2009;75:769–75.
9. Sommers CL, Byers SW, Thompson EW, Torri JA, Gelmann EP. Differentiation state and invasiveness of human breast cancer cell lines. *Breast Cancer Res Treat*. 1994;3:325–35.
10. Foster JS, Henley DC, Bukovsky A, Seth P, Wimalasena J. Multifaceted regulation of cell cycle progression by estrogen: regulation of Cdk inhibitors and Cdc25A independent of cyclin D1-Cdk4 function. *Mol Cell Biol*. 2001;21:794–810.
11. Valgeirsdóttir S, Claesson-Welsh L, Bongcam-Rudloff E, Hellman U, Westermark B, Heldin CH. PDGF induces reorganization of vimentin filaments. *J Cell Sci*. 1998;111:1973–80.
12. Humphries MJ. Cell substrate adhesion assays. In: Bonifacino JS, Dasso M, Harford JB, Lippincott-Schwartz J, Yamada KM, editors. Current protocols in cell biology. Hoboken, New Jersey: John B. Wiley & Sons; 2007:9.1.1–9.1.11.
13. Albini A, Benelli R. The chemoinvasion assay: a method to assess tumor and endothelial cell invasion and its modulation. *Nat Protoc*. 2007;2:504–ll.
14. Akula MR, Collier TL, Kabalka GW, et al. Microfluidic Synthesis of [18F]FLT. *J Nuclear Med*. 2010;51(Suppl 2):294P.
15. Solomon A, Murphy CL, Kestler D, et al. Amyloid contained in the knee joint meniscus is formed from apolipoprotein A-I. *Arthritis Rheum*. 2006;54:3545–50.
16. Ghanem MA, Van der Kwast TH, Sudaryo MK, et al. MIB-1 (KI-67) proliferation index and cyclin-dependent kinase inhibitor p27 (Kip1) protein expression in nephroblastoma. *Clin Cancer Res*. 2004;10:591–7.
17. Sarkar S, Mazumdar A, Dash R, Sarkar D, Fisher PB, Mandal M. ZD6474 enhances paclitaxel antiproliferative and apoptotic effects in breast carcinoma cells. *J Cell Physiol*. 2010;226:375–84.
18. Pellegrin S, Mellor H. Actin stress fibres. *J Cell Sci*. 2007;120:3491–9.
19. Sossey-Alaoui K, Safina A, Li X, et al. Down-regulation of WAVE3, a metastasis promoter gene, inhibits invasion and metastasis of breast cancer cells. *Am J Pathol*. 2007;170:2112–21.
20. Sugano S, Suzuki Y, Ota T, et al. Hypothetical protein FLJ20513 (FLJ20513 mRNA), Accession AK000520, www.ncbi.nlm.nih.gov/; 2000.
21. www.ncbi.nlm.nih.gov/. UniGene: Hs. 143811 Homo sapiens ODAM expression profile.
22. Solomon A, Murphy CL, Weaver K, et al. Calcifying epithelial odontogenic (Pindborg) tumor-associated amyloid consists of a novel human protein. *J Lab Clin Med*. 2003;142:348–55.
23. Murphy CL, Kestler DP, Foster JS, et al. Odontogenic ameloblast-associated protein nature of the amyloid found in calcifying epithelial odontogenic tumors and unerupted tooth follicles. *Amyloid*. 2008;15:89–95.
24. Aung PP, Oue N, Mitani Y, et al. Systematic search for gastric cancer-specific genes based on SAGE data: melanoma inhibitory activity and matrix metalloproteinase-10 are novel prognostic factors in patients with gastric cancer. *Oncogene*. 2006;25:2546–57.

25. Nishio C, Wazen R, Kuroda S, Moffatt P, Nanci A. Disruption of periodontal integrity induces expression of apin by epithelial cell rests of Malassez. *J Periodontal Res*. 2011. In press.
26. Martin TA, Watkins G, Mansel RE, Jiang WG. Loss of tight junction plaque molecules in breast cancer tissues is associated with a poor prognosis in patients with breast cancer. *Eur J Cancer*. 2004;40:2717–25.
27. Liu YN, Lee WW, Wang CY, Chao TH, Chen Y, Chen JH. Regulatory mechanisms controlling human E-cadherin gene expression. *Oncogene*. 2005;24:8277–90.
28. Bauer H, Zweimueller-Mayer J, Steinbacher P, Lametschwandtner A, Bauer HC. The dual role of zonula occludens (ZO) proteins. *J Biomed Biotechnol*. 2011. In press.
29. Zou L, Hazan R, Roy P. Profilin-1 overexpression restores adherens junctions in MDA-MB-231 breast cancer cells in R-cadherin-dependent manner. *Cell Motil Cytoskeleton*. 2009;66:1048–56.
30. Kominsky SL, Argani P, Korz D, et al. Loss of the tight junction protein claudin-7 correlates with histological grade in both ductal carcinoma in situ and invasive ductal carcinoma of the breast. *Oncogene*. 2003;22:2021–33.
31. Radziwill G, Weiss A, Heinrich J, et al. Regulation of c-Src by binding to the PDZ domain of AF-6. *EMBO J*. 2007;26:2633–44.
32. Matter K, Balda MS. Epithelial tight junctions, gene expression and nucleojunctional interplay. *J Cell Sci*. 2007;120:1505–11.
33. Sauermann M, Sahin O, Sültmann H, et al. Reduced expression of vacuole membrane protein 1 affects the invasion capacity of tumor cells. *Oncogene*. 2008;27:1320–6.
34. McSherry EA, McGee SF, Jirstrom K, et al. JAM-A expression positively correlates with poor prognosis in breast cancer patients. *Int J Cancer*. 2009; 125:1343–51.
35. Naik MU, Naik TU, Suckow AT, Duncan MK, Naik UP. Attenuation of junctional adhesion molecule-A is a contributing factor for breast cancer cell invasion. *Cancer Res*. 2008;68:2194–203.
36. Tam CW, Cheng AW, Ma RY, Yao KM, Shiu SY. Inhibition of prostate cancer cell growth by human secreted PDZ domain-containing protein 2, a potential autocrine prostate tumor suppressor. *Endocrinology*. 2006;147:5023–33.
37. Baumgartner M, Radziwill G, Lorger M, Weiss A, Moelling K. c-Src-mediated epithelial cell migration and invasion regulated by PDZ binding site. *Mol Cell Biol*. 2008;28:642–55.
38. Bambang IF, Xu S, Zhou J, Salto-Tellez M, Sethi SK, Zhang D. Overexpression of endoplasmic reticulum protein 29 regulates mesenchymal–epithelial transition and suppresses xenograft tumor growth of invasive breast cancer cells. *Lab Invest*. 2009;89:1229–42.
39. Bühler H, Schaller G. Transfection of keratin 18 gene in human breast cancer cells causes induction of adhesion proteins and dramatic regression of malignancy in vitro and in vivo. *Mol Cancer Res*. 2005;3:365–71.
40. Huang H, Sossey-Alaoui K, Beachy SH, Geradts J. The tetraspanin superfamily member NET-6 is a new tumor suppressor gene. *J Cancer Res Clin Oncol*. 2007;133:761–9.
41. Matsuda Y, Schlange T, Oakeley EJ, Boulay A, Hynes NE. WNT signaling enhances breast cancer cell motility and blockade of the WNT pathway by sFRP1 suppresses MDA-MB-231 xenograft growth. *Breast Cancer Res*. 2009;11:R32.
42. Moffatt P, Smith CE, Sooknanan R, St-Arnaud R, Nanci A. Identification of secreted and membrane proteins in the rat incisor enamel organ using a signal-trap screening approach. *Eur J Oral Sci*. 2006;114(Suppl 1):139–46.
43. Lee HK, Lee DS, Ryoo HM, et al. The odontogenic ameloblast-associated protein (ODAM) cooperates with RUNX2 and modulates enamel mineralization via regulation of MMP-20. *J Cell Biochem*. 2010;111:755–67.
44. Pratap J, Imbalzano KM, Underwood JM, et al. Ectopic runx2 expression in mammary epithelial cells disrupts formation of normal acini structure: implications for breast cancer progression. *Cancer Res*. 2009;69:6807–14.
45. Barnes GL, Hebert KE, Kamal M, et al. Fidelity of Runx2 activity in breast cancer cells is required for the generation of metastases-associated osteolytic disease. *Cancer Res*. 2004;64:4506–13.
46. Javed A, Barnes GL, Pratap J, et al. Impaired intranuclear trafficking of Runx2 (AML3/CBFA1) transcription factors in breast cancer cells inhibits osteolysis in vivo. *Proc Natl Acad Sci U S A*. 2005;102;1454–9.
47. Pratap J, Wixted JJ, Gaur T, et al. Runx2 transcriptional activation of Indian Hedgehog and a downstream bone metastatic pathway in breast cancer cells. *Cancer Res*. 2008;68:7795–802.
48. Coffman JA. Is Runx a linchpin for developmental signaling in metazoans? *J Cell Biochem*. 2009;107:194–202.
49. Shimoyama A, Wada M, Ikeda F, et al. Ihh/Gli2 signaling promotes osteoblast differentiation by regulating runx2 expression and function. *Mol Biol Cell*. 2007;18:2411–8.
50. Ten-Haaf A, Bektas N, von-Serenyi S, et al. Expression of the glioma-associated oncogene homolog (GLI) 1 in human breast cancer is associated with unfavourable overall survival. *BMC Cancer*. 2009;9:298.
51. Xu L, Kwon YJ, Frolova N, et al. Gli1 promotes cell survival and is predictive of a poor outcome in ERalpha-negative breast cancer. *Breast Cancer Res Treat*. 2010;123:59–71.
52. Watkins N, Berman DM, Burkholder SG, Wang B, Beachy PA, Baylin SB. Hedgehog signalling within airway epithelial progenitors and in small-cell lung cancer. *Nature*. 2003;422:313–7.
53. Saqui-Salces M, Merchant JL. Hedgehog signaling and gastrointestinal cancer. *Biochim Biophys Acta*. 2010;1803:786–95.
54. Li X, Decker M, Westendorf JJ. TEThered to Runx: novel binding partners for runx factors. *Blood Cells Mol Dis*. 2010;45:82–5.
55. Li X, Hoeppner LH, Jensen ED, Gopalakrishnan R, Westendorf JJ. Co-activator activator (CoAA) prevents the transcriptional activity of Runt domain transcription factors. *J Cell Biochem*. 2009;108:378–87.
56. Leong DT, Lim J, Goh X, et al. Cancer-related ectopic expression of the bone-related transcription factor RUNX2 in non-osseous metastatic tumor cells is linked to cell proliferation and motility. *Breast Cancer Res*. 2010;12:R89.
57. Nishio C, Wazen R, Kuroda S, Moffatt P, Nanci A. Expression pattern of odontogenic ameloblast-associated and amelotin during formation and regeneration of the junctional epithelium. *Eur Cell Mater*. 2010;20:393–402.

Supplementary materials

Table S1. Hygromycin selection results for recombinant ODAM-expressing clones.

Cell line	Tissue	Number of clones	ODAM-expressing clones
A549	Lung	78	0
Hela	Cervical	71	0
MCF-7	Breast	41	0
T-47D	Breast	35	0
MDA-MB-231	Breast	36	17

Notes: Human tumor cell lines were transfected with eukaryotic expression plasmid PCDNA5T/O containing the full length rODAM open reading frame under control of the CMV promoter and subjected to selection with hygromycin. Resultant clones were tested for ODAM expression by capture ELISA and scored as negative or positive for r-ODAM expression.

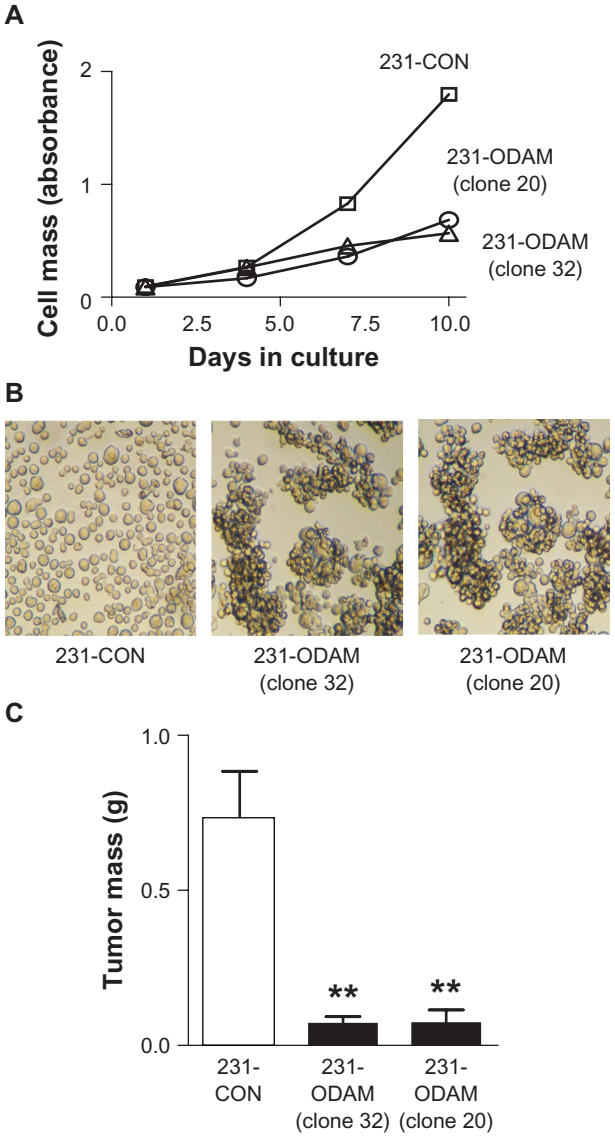

Figure S1. Effects of ODAM expression on growth, aggregation, and tumorigenicity of 2 different stably transfected MDA-MB-231-ODAM clones. **A**) Growth rates of 231-CON (□), 231-ODAM clone #32 (Δ), and 231-ODAM clone #20 (○) cells. Plotted values represent absorbance and are given as mean ± 1 standard deviation for 4 replicates. **B**) Cell aggregation assay for suspension cultures of 231-CON, 231-ODAM clone #32, and 231-ODAM clone #20. **C**) Graphic representation of tumor xenograft masses for 231-CON, 231-ODAM clone #32, and 231-ODAM clone #20 cells 6 wks after implantation into Rag-1 immunodeficient mice. Values represent the averages of tumor masses from 5 mice in each group ± 1 standard deviation (**$P < 0.01$).

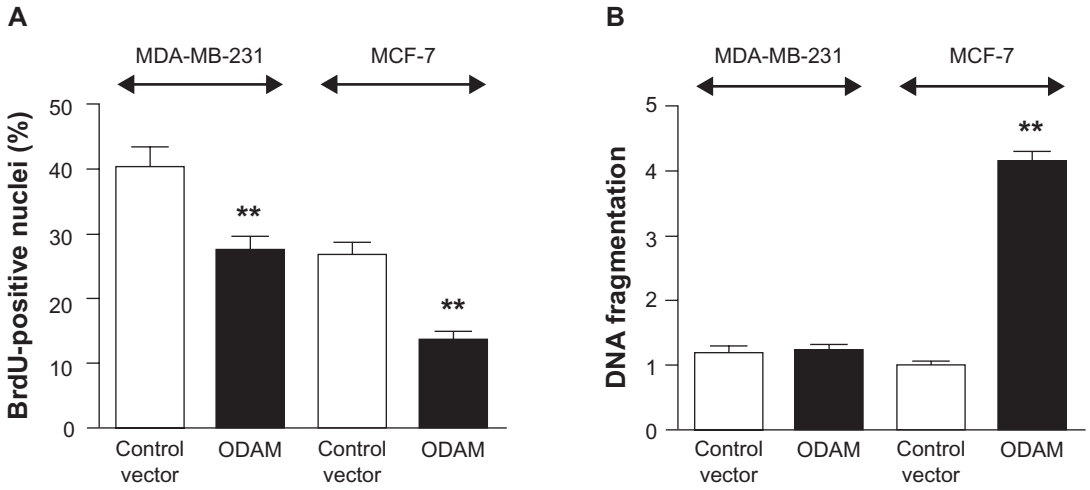

Figure S2. Effects of transient ODAM expression on proliferation and apoptosis in MDA-MB-231 and MCF-7 breast cancer cells. **A**) Proliferation determined from assays of BrdU incorporation at 72 h in transiently transfected cells. Values are given as the mean ± 1 standard deviation of counts from three separate cultures (**$P < 0.01$). **B**) Relative levels of apoptosis in MDA-MB-231 and MCF-7 cells were determined from ELISA measuring soluble chromatin (**$P < 0.01$).